UAV Formation Flight Control Law Utilizing Energy Maneuverability

Jongug Choi* and Youdan Kim**
School of Mechanical and Aerospace Engineering, Seoul National University,
Seoul 151-742, Korea

Gwanyoung Moon***
Agency for Defense Development, Daejeon, Korea

Abstract

This paper deals with the energy saving problem of the follower aircraft in the loose leader-follower formation geometry in which the lateral separation between formation members is more than a wingspan of the leader aircraft. This formation geometry offers no drag benefit, but has a strategic advantage. In the case of loose formation flight, the follower aircraft usually consumes more energy than the leader aircraft because the follower aircraft should use more thrust to maintain given formation geometry, especially during the turning phase from the outside of the leader's flight path or join-up phase. A formation control scheme based on the energy maneuverability is proposed in this paper. To design the proposed control law, the velocity command is designed using feedback linearization for the horizontal formation geometry and then coverts it to the altitude command using the energy equation. Numerical simulation is performed to verify the effectiveness of the proposed controller.

Key Word : Formation flight, Energy conservation, guidance, UAV

Introduction

When aircrafts fly in formation, each aircraft takes advantages of the upwash of air coming off of the aircraft in front of it to reduce its workload. By flying in the area of upwash, a follower aircraft can gain aerodynamic efficiency which leads to energy saving.[1-3] To achieve the energy saving, the follower aircraft must fly in tight formation in which lateral separation between the leader and follower aircraft is less than a wingspan of the leader aircraft.[4] Because of the energy saving effect, several research efforts have been focused on the tight formation flying. In Ref.5, the peak-seeking control scheme was used to optimize the drag benefit during the flight. Ref.4 treated the tight formation maintenance problem for the maneuvering aircraft using linear kinematics. Additionally, non-linear controller was designed taking into account non-linearities that are typical of a formation control dynamics.[6]

Considering the operational requirements to enhance the mutual survivability in threat environment, the tight formation geometry may not be suitable. For example, in case combat aircrafts perform air patrol mission in the threat area, formation geometry is decided based on the surface-to-air and air-to-air threats of the enemy. This tactical formation geometry is loose formation in which the lateral separation between formation members is more than a wingspan of the leader aircraft. This formation geometry offers no drag benefit, but has a strategic advantage.

* Ph.D Candidate
** Professor
E-mail : ydkim@snu.ac.kr Tel : 82-2-880-7398 FAX : 82-2-880-2662
*** Researcher, Ph.D

In the case of loose formation flight, the follower aircraft usually consumes more energy than the leader aircraft because the follower aircraft should use more thrust to maintain given formation geometry, especially during the turning phase from the outside of the leader's flight path or join-up phase.

This paper addresses the energy saving problem of the follower aircraft in the loose formation, especially a formation control scheme based on the energy maneuverability is proposed. This idea was adopted from the energy maneuverability method in Ref.7. Usually, the dogfight maneuvers of high performance jet fighters rely upon the exchange of potential and kinetic energy to obtain a positional advantage. For example, the "High Speed Yo-Yo" maneuver is used to overtake a slower aircraft in a hard turn. The attacker pulls up, trading kinetic energy for potential energy and slowing to allow a higher turn rate. After the turning, the attacker rolls for partially inverted and pulls down astern of the opponent, exchanging the potential energy back for speed. This skill is used for formation flight in this study. In energy maneuverability, the kinetic and potential energy are exchanged to achieve desired speed or height. Thus, the thrust is only required to balance the energy dissipated by the aerodynamic drag along the path.

In this study, it is assumed that the formation is composed of two aircrafts and the leader aircraft performs steady state level flight. To design the proposed control law, the velocity command for the follower aircraft is designed using feedback linearization for the horizontal formation geometry[6] and then coverts it to the altitude command using the energy equation.

The paper is organized as follows: Section 2 deals with system modeling, formation geometry and formation flight method using the energy maneuverability. Section 3 describes the control design problem. Feedback linearization method is used to generate a follower command. The autopilots are designed using the sliding mode control scheme for vertical control channel and PI controller for horizontal control channel, respectively. Numerical simulation results are shown in Sec. 4 to verify the performance of the proposed method. Finally, conclusions are given in Sec.5.

Problem Formulation

2.1 System Dynamics

In this study, three dimensional point mass model is considered for aircraft dynamics.

$$\dot{X}_i = V_i \cos(\gamma_i)\cos(\chi_i) \tag{1}$$

$$\dot{Y}_i = V_i \cos(\gamma_i)\sin(\chi_i) \tag{2}$$

$$\dot{h}_i = V_i \sin(\gamma_i) \tag{3}$$

$$\dot{V}_i = g\left(\frac{T_i - D_i}{W_i} - \sin\gamma_i\right) \tag{4}$$

$$\dot{\gamma}_i = \frac{-g\cos\gamma_i + g}{V_i} + \frac{a_{p_i}}{V_i} \tag{5}$$

$$\dot{\chi}_i = \frac{a_{y_i}}{V_i} \tag{6}$$

where X_i and Y_i are x-direction and y-direction position variables, h_i denote the height, V_i is the velocity, γ_i and χ_i are the flight path and heading angles, respectively. Note that $i=1$ represents the leader, and $i=2$ represents the follower aircraft. It is assumed that the flight path angle γ_1 of the leader vehicle is zero. And T_i is the thrust, D_i is the aerodynamic drag, W_i is the weight of each aircraft, and g is a gravitation constant. The above equation can be obtained with the assumptions of constant weight, point-mass aircraft with thrust aligned along the velocity vector, flat non-rotating Earth, and constant gravitational attraction.

The thrust and aerodynamic drag are modeled as[8]

$$T_i = \eta_i T_{\max} \tag{7}$$

$$D_i = D_{0i} + n_i^2 D_{ii} \tag{8}$$

where η_i is throttle value, $T_{\max}$ is maximum thrust, D_{0i} is parasite drag, D_{ii} is induced drag and n_i is load factor. In Eqs. (7) and (8), the throttle value η_i, the induced drag D_{ii} and the parasite drag D_{0i} can be represented as

$$\dot{\eta}_i = -\frac{1}{\tau_\eta}\eta_i + \frac{1}{\tau_\eta}\eta_{ci},\ 0 \le \eta_{ci} \le 1 \tag{9}$$

$$D_{0i} = q_i S C_{D_0},\ D_{ii} = k(W/q_i S)^2 \tag{10}$$

where τ_η is non-dimensional engine time constant, q_i is dynamic pressure, S is wing area, C_{D_0} is zero-lift drag coefficient, and k is drag polar constant.

Consequently, the control variables in this study are throttle command η_{ci}, pitch acceleration a_{pi}, and yaw acceleration a_{yi}.

2.2 Formation Geometry

Fig. 1 shows the Leader/Wingman configuration considered in this study. To maintain the formation geometry, the follower aircraft must keep its prescribed relative position with respect to the leader aircraft. Earth-fixed coordinate is considered as the inertial coordinate, and the body-fixed coordinate is attached to the cg position of the leader. The flight path of the formation flight usually lies on a horizontal plane, and therefore, it can be assumed that $\gamma_i \approx 0$. The formation flight control problem can be decomposed into two decoupled problems, the horizontal tracking problem and vertical tracking problem.

The parameters of the formation geometry are the forward clearance x_d, lateral clearance y_d, and the vertical distance clearance h_d from the reference frame of the leader, as shown in Fig. 1 The forward distance error e_x and lateral distance error e_y in an inertial coordinate frame can be expressed as

$$e = \begin{bmatrix} X_1 - X_2 \\ Y_1 - Y_2 \end{bmatrix} - T(\chi_1)\begin{bmatrix} x_d \\ y_d \end{bmatrix} \tag{11}$$

where χ_1 and $T(\chi_1)$ represent the heading angle of the leader aircraft and rotation matrix, respectively. The rotation matrix is

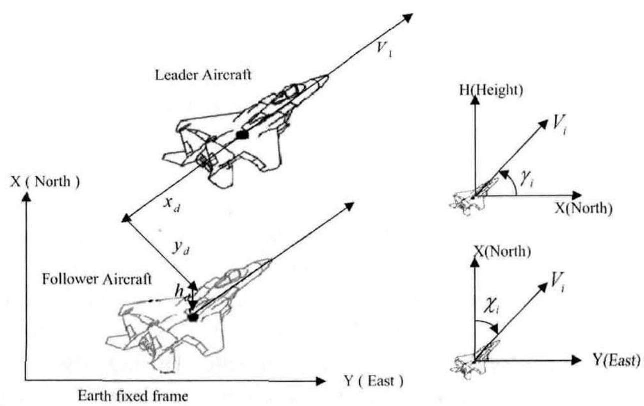

Fig. 1. Formation Geometry

$$T(\chi_1) = \begin{bmatrix} \cos\chi_1 & -\sin\chi_1 \\ \sin\chi_1 & \cos\chi_1 \end{bmatrix} \tag{12}$$

The vertical distance error e_h can be represented as

$$e_h = h_1 - h_2 - h_d \tag{13}$$

The specific energy error e_E can be defined as

$$e_E = E_{d2} - E_2 \tag{14}$$

where $E_{d2} = f(V_1, h_1, h_d)$ is the desired energy state.

2.2 Energy Maneuverability based formation flight

The specific energy of a point mass aircraft is the sum of the potential and kinetic energy as follows [7]

$$E = h + \frac{1}{2g} V^2 \tag{15}$$

The specific energy has unit of distance and is also called "energy height" because it equals to the altitude that the aircraft can reach. Power is the time rate of energy usage, and therefore the "specific power" can be defined as

$$P_{s_{used}} = \frac{E}{dt} = \frac{dh}{dt} + \frac{V}{g}\frac{dV}{dt} \tag{16}$$

The specific power equals to the following "specific excess power"

$$P_s = V\left(\frac{T-D}{W}\right) = \frac{dh}{dt} + \frac{V}{g}\frac{dV}{dt} \tag{17}$$

If P_s equals to zero, the drag of the aircraft equals to the thrust, and there is no excess power. Of course, this does not always mean that the aircraft is in the level flight with constant speed. However, if the sum of the energy usage equals to zero, then the aircraft must be in the level flight with constant speed, or a climb flight with decelerating, or a descend flight with accelerating.

Energy maneuverability involves the specification of aircraft climb and/or acceleration capability for various combination of speed, altitude, and turning load factor. In other words, the potential energy can be exchanged with the kinetic energy to achieve the desired speed or height[7].
From Eqs. (3) and (16), P_{si} can be represented as

$$P_{si} = V_i(\sin\gamma_i + \dot{V}_i/g) \tag{18}$$

Assuming that the same energy level is maintained during flight, the following equation can be obtained for constant energy level case, i.e., $P_{si} = 0$.

$$\dot{V}_i = -g\sin\gamma_i \tag{19}$$

Note from Eq. (19) that the velocity can be changed by using the flight path angle. This means that the aircraft must be in a level flight with constant speed, or in a climb while decelerating, or in a descent while accelerating to maintain a specified energy level. In other words, the velocity regulating the forward distance error can be obtained by exchanging the potential energy with the kinetic energy of the aircraft. During the energy transformation, however, some energy may be dissipated by the aerodynamic drag. To compensate this energy loss, the throttle is used to maintain the energy level in this study.

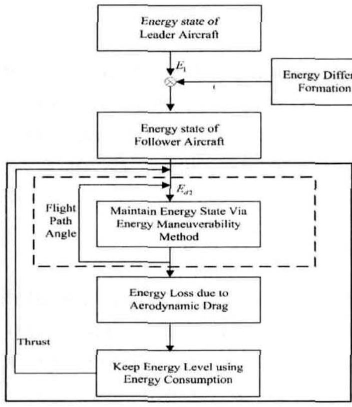

Fig. 2. Schematic Diagram of Proposed Control Concept

Let us consider the case that the follower aircraft is required to have V_{c2} to reduce the forward distance error e_x and the follower aircraft maintains the desired formation geometry using energy maneuverability during formation flight. Then the follower aircraft has to approach the desired altitude h_{d2} by using the flight path angle while regulating the specific energy error e_E. The desired altitude is obtained from the desired energy state E_{d2} and V_{c2} as

$$h_{d2} = E_{d2} - \frac{V_{c2}^2}{2g} \tag{20}$$

where the desired energy state can be calculated from the leader's velocity, heading information and the vertical distance clearance h_d from the reference frame of the leader as

$$E_{d2} = h_1 + \frac{V_1^2}{2g} + h_d \tag{21}$$

Fig. 2 shows the schematic diagram of the proposed control concept.

Control Design

The control system of each aircraft consists of the command generator and autopilot, as shown in Fig. 3. The command generator generates command signals to track the desired trajectory. The command generator of the leader aircraft generates command signals without using the energy maneuverability scheme, but that of the follower aircraft generates command signals using the energy maneuverability method. The autopilot of each aircraft is designed using the sliding mode control for the vertical control channel and the PID control for the horizontal control channel. The detailed design process is explained in the following section.

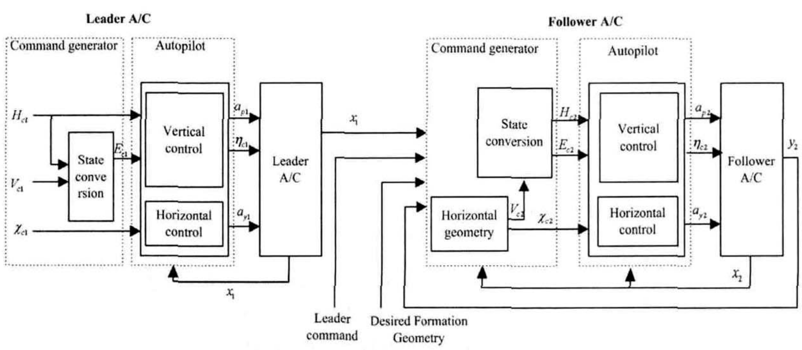

Fig. 3. Control Configuration

3.1 Command Generator

The command generator of the leader aircraft generates command signals without using the energy maneuverability method. It is assumed that the command generator of the leader aircraft can generate the proper command signals to track the desired reference trajectory. The velocity command signal V_{c1} is converted to the energy command signal E_{c1} as

$$E_{c1} = H_{c1} + \frac{V_{c1}}{2g} \tag{22}$$

The objective of the command generator of the follower aircraft is to maintain the relative distance between the aircrafts close to the desired value. To design the command generator of the follower aircraft, feedback linearization method is used to produce V_{c2} and χ_{c2}.[6] And the velocity command V_{c2} is converted to h_{c2} and E_{c2} by using Eqs. (20) and (21) by applying the concept of the energy maneuverability method. The command generator of the follower aircraft consists of two blocks, the "state conversion" block and the "horizontal geometry" block. The "state conversion"block provides the desired energy command E_{c2} and altitude command h_{c2} to the autopilot as.

$$E_{c2} = h_1 + \frac{V_1^2}{2g} + h_d \tag{23}$$

$$h_{c2} = E_{c2} - \frac{V_{c2}^2}{2g} \tag{24}$$

The feedback linearization based controller is designed for the "horizontal geometry" block that takes the lateral and forward errors as inputs. This block calculates the desired velocity V_{c2} and heading angle command χ_{c2}, and sends these commands to the "state conversion" and "autopilot" blocks, respectively. To design the command generator, simple UAV dynamics with autopilot is used. The autopilot dynamics is assumed as the following first order filters

$$\dot{V}_i = -\lambda_V (V_i - V_{ci}) \tag{25}$$

$$\dot{\chi}_i = -\lambda_\chi (\chi_i - \chi_{ci}) \tag{26}$$

The first and second derivatives of the Eq. (11) can be written as

$$\dot{e} = \begin{bmatrix} \dot{X}_1 - \dot{X}_2 \\ \dot{Y}_1 - \dot{Y}_2 \end{bmatrix} - \begin{bmatrix} -\sin\chi_1 & -\cos\chi_1 \\ \cos\chi_1 & -\sin\chi_1 \end{bmatrix} \dot{\chi}_1 \tag{27}$$

$$\ddot{e} = \begin{bmatrix} \ddot{X}_1 - \ddot{X}_2 \\ \ddot{Y}_1 - \ddot{Y}_2 \end{bmatrix} + \begin{bmatrix} \cos\chi_1 & -\sin\chi_1 \\ \sin\chi_1 & \cos\chi_1 \end{bmatrix} \begin{bmatrix} x_d \\ y_d \end{bmatrix} \dot{\chi}_1^2 - \begin{bmatrix} -\sin\chi_1 & -\cos\chi_1 \\ \cos\chi_1 & -\sin\chi_1 \end{bmatrix} \begin{bmatrix} x_d \\ y_d \end{bmatrix} \ddot{\chi}_1 \tag{28}$$

where

$$\dot{X}_i = V_i \cos\gamma_i \cos\chi_i, \quad \dot{Y}_i = V_i \cos\gamma_i \sin\chi_i, \quad i = 1,2 \tag{29}$$

The flight path angle is assumed as $\gamma_i \approx 0$, and therefore, Eq. (29) can be written as

$$\dot{X}_i = V_i \cos\chi_i, \quad \dot{Y}_i = V_i \sin\chi_i \tag{30}$$

Differentiating Eq. (30) gives

$$\begin{aligned} \ddot{X}_i &= \dot{V}_i \cos\chi_i - V_i \sin\chi_i \dot{\chi}_i \\ \ddot{Y}_i &= \dot{V}_i \sin\chi_i + V_i \cos\chi_i \dot{\chi}_i \end{aligned} \tag{31}$$

It is assumed that the leader aircraft is performing a steady-state turn, and therefore $\ddot{\chi}_1 = 0$ in Eq.(28). This assumption is reasonable and acceptable in autonomous formation flight situations such as cruise formation or way point passing flight with steady coordinated turn. Now, from Eqs.(25) and (26), Eq.(28) can be rewritten as

$$\ddot{e}=f+Gu \tag{32}$$

where

$$u=[V_{c2} \ \ \chi_{c2}]^T$$

$$f=\begin{bmatrix}\ddot{X}_1+\lambda_v V_2\cos\chi_2-V_2\sin\chi_2\lambda_\chi\chi_2\\ \ddot{Y}_1+\lambda_v V_2\sin\chi_2+V_2\cos\chi_2\lambda_\chi\chi_2\end{bmatrix}+\begin{bmatrix}\cos\chi_1 & -\sin\chi_1\\ \sin\chi_1 & \cos\chi_1\end{bmatrix}\begin{bmatrix}x_d\\ y_d\end{bmatrix}\dot{\chi}_1^2$$

$$G=\begin{bmatrix}-\lambda_v\cos\chi_2 & \lambda_\chi V_2\sin\chi_2\\ -\lambda_v\sin\chi_2 & -\lambda_\chi V_2\cos\chi_2\end{bmatrix}$$

It can be easily shown that $\det G=\lambda_v\lambda_\chi V_2$. Hence, the controller for the system Eq. (32) can be designed using the feedback linearization for all $V_2(t)\neq 0$ as[6]

$$u=G^{-1}\left[-f-k_1\dot{e}-k_2 e\right] \tag{33}$$

where $k_1, k_2>0$ are the design parameters to obtain the desired error dynamics.

3.2 Autopilot

The objective of the autopilot is to design $[a_{pi}\ \eta_{ci}\ a_{yi}]$ to track the command signal $[h_{ci}\ E_{ci}\ \chi_{ci}]$. The same control system structures of the leader and the follower aircraft are considered in this study. The autopilot is composed of two channels, a "horizontal control" channel and "vertical control" channel, as shown in Fig. 3. The "vertical control" channel provides control η_{ci}, a_{pi} to track the energy command E_{ci} and the altitude command h_{ci}. The "horizontal control" channel provides a_{yi} to track the heading angle command χ_i.

The "vertical control" channel is designed by using the sliding control method. The output dynamics for energy state E_i and altitude h_i of each aircraft can be derived by differentiating Eqs. (3) and (18) as

$$\ddot{E}_i=f_{Ei}+b_{Ei}\eta_{ci} \tag{34}$$

$$\ddot{h}_i=f_{hi}+b_{hi}a_{pi} \tag{35}$$

where

$$f_{Ei}=\frac{1}{W_i}\left(\left(\frac{\partial V_i}{\partial E_i}(T_i-D_i)-\frac{\partial D_i}{\partial E_i}V_i\right)\frac{V_i(T_i-D_i)}{W_i}+\left(\frac{\partial V_i}{\partial h_i}(T_i-D_i)-\frac{\partial D_i}{\partial h_i}V_i\right)V_i\sin\gamma_i+\frac{\partial T_i}{\partial \eta_i}V_i\right) \tag{36}$$

$$f_{hi}=\frac{\partial V_i}{\partial E_i}\frac{V_i(T_i-D_i)}{W_i}sin\gamma_i+\frac{\partial V_i}{\partial h_i}V_i\sin^2\gamma_i-g\cos^2\gamma_i \tag{37}$$

$$b_{Ei}=\frac{V_i}{W_i}\frac{\partial T_i}{\partial \eta_i}\ ,\quad b_{hi}=\cos\gamma_i \tag{38}$$

$$\frac{\partial V_i}{\partial E_i}=\frac{g}{V_i}\ ,\quad \frac{\partial D_i}{\partial E_i}=\rho_i g S_i C_{D_o}-\frac{n_i^2 k_i W_i^2}{2(\rho_i g S_i)^2(E_i-h_i)^3} \tag{39}$$

$$\frac{\partial V_i}{\partial h_i}=-\frac{g}{V_i}=-\frac{\partial V_i}{\partial E_i}\ ,\quad \frac{\partial D_i}{\partial h_i}=-\rho_i g S_i C_{D_o}+\frac{n_i^2 k_i W_i^2}{2(\rho_i g S_i)^2(E_i-h_i)^3}=-\frac{\partial D_i}{\partial E_i} \tag{40}$$

Let us define the sliding surface as

$$s_{Ei}=\left(\frac{d}{dt}+\lambda_{Ei}\right)^2\int_0^t e_{Ei}(\tau)d\tau\ ,\quad e_{Ei}(\tau)=E_i-E_{ci} \tag{41}$$

$$s_{hi}=\left(\frac{d}{dt}+\lambda_{hi}\right)^2\int_0^t e_{hi}(\tau)d\tau\ ,\quad e_{Ei}(\tau)=h_i-h_{ci} \tag{42}$$

where λ_{Ei} and λ_{hi} are positive constants that are related to the band-width of the error dynamics. Differentiating s_{Ei} and s_{hi}, we have

$$\dot{s}_{Ei} = -\ddot{E}_{ci} + f_{Ei} + 2\lambda_{Ei}\dot{e}_{Ei} + \lambda_{Ei}^2 e_{Ei} + b_{Ei}\eta_{ci} \tag{43}$$

$$\dot{s}_{hi} = -\ddot{h}_{ci} + f_{hi} + 2\lambda_{hi}\dot{e}_{hi} + \lambda_{hi}^2 e_{hi} + b_{hi}a_{pi} \tag{44}$$

Above equations can be rewritten in a compact form as

$$\begin{bmatrix} \dot{s}_{Ei} \\ \dot{s}_{hi} \end{bmatrix} = \begin{bmatrix} \nu_{Ei} \\ \nu_{hi} \end{bmatrix} + \begin{bmatrix} b_{Ei} & 0 \\ 0 & b_{hi} \end{bmatrix} \begin{bmatrix} \eta_{ci} \\ a_{pi} \end{bmatrix} \tag{45}$$

where

$$\nu_{Ei} = -\ddot{E}_{ci} + f_{Ei} + 2\lambda_{Ei}\dot{e}_{Ei} + \lambda_{Ei}^2 e_{Ei} \tag{46}$$

$$\nu_{hi} = -\ddot{h}_{ci} + f_{hi} + 2\lambda_{hi}\dot{e}_{hi} + \lambda_{hi}^2 e_{hi} \tag{47}$$

Now, the control inputs can be determined such that the following sliding conditions are satisfied:

$$\frac{1}{2}\frac{d}{dt}s_{Ei}^2 \le -k_{Ei}|s_{Ei}| \tag{48}$$

$$\frac{1}{2}\frac{d}{dt}s_{hi}^2 \le -k_{hi}|s_{hi}| \tag{49}$$

where k_{Ei} and k_{hi} are positive constants. The controller that satisfies the sliding conditions (48) and (49) can be determined as

$$\begin{bmatrix} \eta_{ci} \\ a_{pi} \end{bmatrix} = B_i^{-1} \begin{bmatrix} -\nu_{Ei} - k_{Ei}\,sat\left(\dfrac{s_{Ei}}{\Phi_{Ei}}\right) \\ -\nu_{hi} - k_{hi}\,sat\left(\dfrac{s_{hi}}{\Phi_{hi}}\right) \end{bmatrix}, \quad B_i = \begin{bmatrix} b_{Ei} & 0 \\ 0 & b_{hi} \end{bmatrix} \tag{50}$$

where Φ_{Ei}, Φ_{hi} are the widths of the boundary layer. Note from Eqs.(38),(50) that the inverse of B_i does exist for the entire flight envelop except for $V_i = 0$ or $\gamma_i = 90^\circ$, which are not unusual flight condition.

The "horizontal control" channel is a linear heading controller. The controller is designed using the PI control method in this study as

$$a_{yi} = k_{\chi_\pi} e_{\chi_i} + k_{\chi_I}\int e_{\chi_i}, \quad e_{\chi_i}(\tau) = \chi_{ci} - \chi_i \tag{51}$$

Remarks :

(i) In the proposed control scheme, the follower aircraft should change the altitude to maintain a given formation pattern. Therefore, the altitude command should be limited inside the flight envelop by considering the minimum altitude and safe altitude.

$$h_{2\min} < h_{c2} < h_2(V_{2stall}) \tag{52}$$

where $h_2(V_{2stall})$ can be calculated as

$$h_2(V_{2stall}) = E_2 - \frac{V_{2stall}^2}{2g} \tag{53}$$

(ii) The proposed control scheme will be proper at the cases that does not require altitude clearance constraint. So the proper cases are join-up phase for mission or combat air patrol mission.

SIMULATION

Numerical simulation was performed to evaluate the performance of the proposed controller(Control 1). The initial positions of the leader and the follower are $[0\ 0\ 1000]m$ and $[-50\ 0\ 1000]m$, respectively. The initial speeds of the leader and the follower are 100 m/sec. The leader maintained the steady level flight condition with velocity of 100m/s. The desired relative distance (x_d, y_d, h_d) of the follower is $[1\ 50\ 0]m$. The desired relative distance signals are generated by the second order filter with natural frequency(ω_n)=0.05 rad/sec and damping ratio(ξ)=1.

For comparison, another reference controller which does not use the energy maneuverability is designed(Control 2). The Control 2 is composed of the command generator for generating the speed and heading command signals, and the command generator for generating the following

$$E_{c2_{woEM}} = h_i + \frac{V_{c2}^2}{2g} + h_d\ ,\quad h_{c2_{woEM}} = h_1 + h_d \tag{54}$$

Note that Eq.(54) does not reflect the kinetic and potential energy exchange.

Aircraft parameters used in the simulation are listed in Table 1 [8]. And the control parameters used in the simulation of the command generator and the autopilot are summarized in Table 2.

Table 1. Parameters in the simulation

Parameter	Notation	Value
Wing area	S	27.87
Zero-lift drag coefficient	C_{D_0}	0.015
Drag polar constant	k	0.02
Maximum lift coefficient	$C_{L_{max}}$	1.5
Mass	m	11,336.4 kg
Maximum thrust without after burner	T_{max}	6,500 kg
Speed limit	V_{stall}	90 m/s

Table 2. Command generator and autopilot parameters

Parameter	Leader aircraft	Follower aircraft
Command Generator	Do not consider	$\lambda_v = 5\ ,\ \lambda_\chi = 10$ $k_1 = 4I_2,\ k_2 = 4I_2$
Vertical Control	$\lambda_{E1} = 5,\ k_{E1} = 0.1,\ \Phi_{E1} = 1$ $\lambda_{h1} = 5,\ k_{h1} = 0.1,\ \Phi_{h1} = 0.$	$\lambda_{E2} = 5,\ k_{E2} = 0.1,\ \Phi_{E2} = 1$ $\lambda_{h2} = 5,\ k_{h2} = 0.1,\ \Phi_{h2} = 0.$
Heading controller	$k_{\chi_{p1}} = 100,\ k_{\chi_{I1}} = 1$	$k_{\chi_{p2}} = 100,\ k_{\chi_{I2}} = 1$

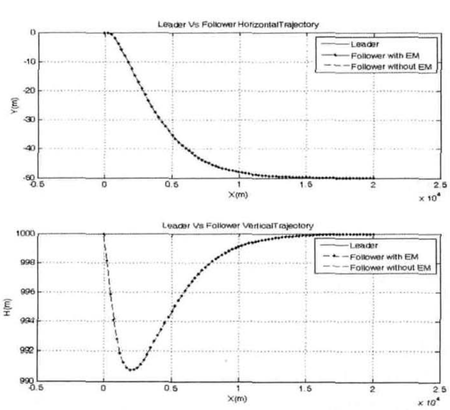

Fig. 4. Leader and Follower Trajectories

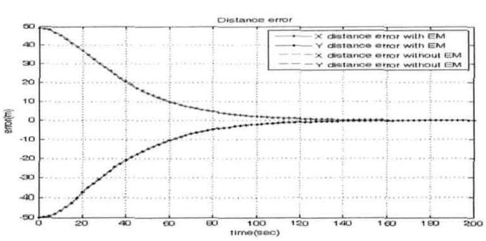

Fig. 5. Horizontal Distance Error Histories

Table 3. Total energy and thrust usage

	Control 1	Control 2
Total Energy($\int_0^t Edt$)	302042	302543
Total Thrust($\int_0^t Tdt$)	514680	514691

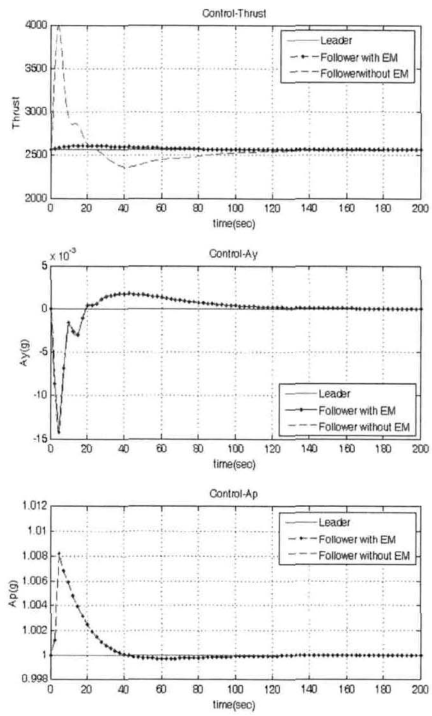

Fig. 6. Control Histories

The simulation results are shown in Figs. 4-6. Figure 4 shows the trajectory histories of the two controller. As shown in fig.4, control 1 performs the energy maneuverability(EM) at the initial phase. The follower aircraft descends from 1000ft to 991ft to exchange the energy. Figure 5 shows the horizontal distance error histories. The horizontal errors have almost same values for the two controllers. Figure 6 shows the control histories. The thrust of the control 1 have less than that of control 2 and more moderate thrust usage.

The total energy and thrust usage are summerized at the table 3. The total energy and thrust usage of the control 1 less than those of the control 2 as shown in table 3.

CONCLUSION

In this paper, formation flight controller based on the energy maneuverability concept is proposed. Numerical simulation was performed to verify the effectiveness of the proposed method. The result of the numerical simulation showed that the energy usage and thrust usage using EM method was less than that without using EM method at the loose formation geometry. Note that the proposed controller forces the follower aircraft to change its altitude to maintain formation geometry. Therefore, the proposed controller may be useful for the formation geometry that requires a large relative distance between the leader and follower aircraft than for the tight formation geometry.

ACKNOWLEDGMENTS

This work was supported by the Korea Science and Engineering Foundation(KOSEF) grant funded by the Korea government(MOST) (No. R0A-2007-000-10017-0).

REFERENCES

1. Hummel, D., "The Use of Aircraft Wakes to Achieve Power Reductions in Formation Flight", The Characterisation & Modification of Wakes from Lifting Vehicles in Fluids, AGARD Conference Proceedings 584, The Advisory Group for Aerospace Research and Development, Neuilly-sur-Seine, France, 1996, pp. 36.1 - 36.13.

2. Wagner, G., Jacqeus, D., Blake, W., and Pachter, M., " Flight Test Results of Close Formation Flight For Fuel Savings", AIAA Atmospheric Flight Mechanics Conference and Exhibit, Monterey, CA, USA, August 2002.

3. Wagner, G., Jacqeus, D., Blake, W., and Pachter, M., " An Analytical Study of Drag Reduction in Tight Formation Flight", AIAA Atmospheric Flight Mechanics Conference and Exhibit, Montreal, Qebec, Canada, August 2001.

4. Pachter, M., D'Azzo, J. J., and Proud, A. W., "Tight Formation Flight Control", Journal of Guidance, Control, and Dynamics,Vol. 24, No. 2, 2001, pp. 246 - 254.

5. Chichka, D. F., Speyer, J. L., Fanti, D., and Park, C. G., "Peak-Seeking Control for Drag Reduction in Formation Flight", Journal of Guidance, Control, and Dynamics, Vol. 29, No. 5, 2006, pp. 1221-1230.

6. Boskovic, J. D., Li, S. M., and Mehra, R. K., "Semi-Globally Stable Formation Flight Control Design in Three Dimensions", Proceedings of the 40th IEEE Conference on Decision and Control, Orlando, FL, USA, December 2001.

7. Raymer, D. P., Aircraft Design : A Conceptual Approach, AIAA, Washington, DC, 1989, chaps.3,17,appendix A.4-2.

8. Segal, S., Ben-Asher, J. Z., and Weiss, H., "Derivation of Formation - Flight Guidance Laws for Unmanned Air Vehicles", Journal of Guidance, Control, and Dynamics, Vol. 28, No. 4, 2005, pp. 733-742.